



**HAL**  
open science

# Design of Speed Sensorless Control of Induction Motor Based on Dual-Nonlinear Control Technique

Abdelkarim Ammar, Tarek Ameid, Younes Azzoug, Aissa Kheldoun, Brahim  
Metidji

► **To cite this version:**

Abdelkarim Ammar, Tarek Ameid, Younes Azzoug, Aissa Kheldoun, Brahim Metidji. Design of Speed Sensorless Control of Induction Motor Based on Dual-Nonlinear Control Technique. 2020 International Conference on Electrical Engineering (ICEE), Sep 2020, Istanbul, Turkey. pp.1-6, 10.1109/ICEE49691.2020.9249796 . hal-04294408

**HAL Id: hal-04294408**

**<https://univ-artois.hal.science/hal-04294408v1>**

Submitted on 20 Nov 2023

**HAL** is a multi-disciplinary open access archive for the deposit and dissemination of scientific research documents, whether they are published or not. The documents may come from teaching and research institutions in France or abroad, or from public or private research centers.

L'archive ouverte pluridisciplinaire **HAL**, est destinée au dépôt et à la diffusion de documents scientifiques de niveau recherche, publiés ou non, émanant des établissements d'enseignement et de recherche français ou étrangers, des laboratoires publics ou privés.

Copyright

# Design of Speed Sensorless Control of Induction Motor Based on Dual-Nonlinear Control Technique

Abdelkarim AMMAR<sup>1,2,\*</sup>, Tarek Ameid<sup>3</sup>, Younes AZZOUG<sup>2,3</sup>, Aissa KHELDOUN<sup>1</sup>, Brahim METIDJI<sup>1</sup>

<sup>1</sup>Signals and Systems Laboratory (LSS), Institute of Electrical and Electronic Engineering, University of M'hamed BOUGARA of Boumerdes, Boumerdes, Algeria.

<sup>2</sup>LGEB Laboratory, Electrical Engineering Department, Biskra University, Algeria

<sup>3</sup> Faculty of Applied Science, Univ. Artois, EA 4025 LSEE F-62400, Béthune, France.

a.ammar@univ-boumerdes.dz, tarek.ameid@ieec.org, azzougyounes@yahoo.fr, aissa1973@gmail.com, metidji77@yahoo.fr

## Abstract

This paper deals with performance improvement of direct flux and torque control of induction motor. The proposed algorithm consists of the combination of two nonlinear control approaches. A decoupled control design is done by the exact feedback linearization control. Since, wastes the control stability and robustness while the presence of disturbance and modeling inaccuracy, it is recommended to be associated with a robust control approach like second-order sliding mode control (SOSMC). Therefore, the super twisting algorithm is integrated as auxiliary inputs to the feedback linearization control law to achieve robust feedback linearization control. On the other hand, the high-performance control design requires accurate knowledge of different control variables such as stator flux and rotor speed. Instead of using costly and fragile sensors that may increase the volume and decrease the reliability of the control system, a proposed sliding super twisting observer and model reference adaptive system serves as sensorless algorithms for rotor speed and flux estimation in wide speed region. This conjunction is intended to enhance the overall control performances and speed/flux estimation, especially at low-speed operations. An experimental study has been done using MATLAB/Simulink with dSpace 1104 real-time interface for investigating the performance of the proposed algorithms.

**Keyword:** Induction Motor, Feedback linearization, Super twisting algorithm, Sliding mode observer, dSpace 1104

## I. INTRODUCTION

Nowadays, the new variable frequency drives like direct torque control (DTC) and Field oriented control become viable and offer a simple structure, effective decoupled control and fast dynamics [1]. However, the conventional techniques like FOC [2] and DTC-SVM [3] use linear proportional-integral (PI) which cannot be sufficient to deal with a high degree of uncertainty like the nonlinear coupling of the machine, external disturbances or parameters variation [4]. Moreover, they base on a non-stationary frame which increases the complexity of control's algorithm by requesting coordinates transformation.

To solve these problems and ensure a perfect decoupling, various control methods are presented for this context, we mention the artificial intelligence techniques and nonlinear control approaches [5]. The most popular nonlinear control method are backstepping, feedback linearization control and sliding mode control (SMC) [6]. The feedback linearization is a nonlinear control technique that can achieve a good performance decoupled control system. It bases on the

conversion of a nonlinear system into a linear one to make it more appropriate for control design [7]. However, the application of feedback linearization is limited only to systems which have a well-defined model. In addition, its stability and robustness cannot be guaranteed while the presence of uncertainties [8]. The combination of the feedback linearization with the sliding mode control (SMC) has been presented in [9], where the sliding mode control is applied on the resulting linearized system which is obtained by feedback linearization. This combination can handle the sensitivity of the system due to parameters variation. However, the disagreeable chattering phenomenon of the conventional SMC causes an infinite commutation which excites high harmonics [10]. The second order sliding mode control has been presented as an alternative to mitigate the effect of chattering. The continuous super twisting algorithm control law is able to reduce the effect of chattering and keep the same desired features of the conventional sliding mode control [4]. The main advantage of the super twisting algorithm (STA) is that it does not require the time derivatives of the sliding variable. This technique can provide a continuous control law by using only the information on the sliding surface [11].

The application of advanced closed control needs an accurate speed and flux measurement or estimation. The use of sensors for measurement is accompanied by several problems, such as cost, fragility and installation. As an alternative, the sensorless control can reduce overall cost and size of the electric drive system and improve its reliability by, the elimination of sensors. The sliding mode control approach proves its worth in this field, whereas it is applicable for both, observers and controllers design. The sliding mode observers (SMOs) are known by their robustness and simplicity [11], [12]. In this work, a second-order super twisting observer is proposed for speed and flux reconstruction. The super twisting observer can compensate the chattering effect and improve speed estimation in low-speed region.

The main propose of this work is to enhanced induction motor control using two nonlinear approaches. A feedback linearization and super twisting incorporation to confront different challenges during motor operation. Moreover, a super twisting observer for speed and flux estimation in a wide speed region serves as a sensorless algorithm. The effectiveness of the proposed dual nonlinear control has been checked through experimental implementation using MATLAB/Simulink software with the aid of dSpace 1104 real-time interface

## II. INDUCTION MACHINE MATHEMATICAL MODEL

The dynamic equations of the induction motor are given in (1) in the stationary reference frame:

$$\begin{cases} \dot{i}_{s\alpha} = -\mu i_{s\alpha} - \omega_r i_{s\beta} + \frac{1}{\sigma L_r} \left( \frac{\psi_{s\alpha}}{T_s} + \omega_r \psi_{s\beta} \right) + \frac{V_{s\alpha}}{\sigma L_s} \\ \dot{i}_{s\beta} = -\mu i_{s\beta} + \omega_r i_{s\alpha} + \frac{1}{\sigma L_r} \left( \frac{\psi_{s\beta}}{T_s} - \omega_r \psi_{s\alpha} \right) + \frac{V_{s\beta}}{\sigma L_s} \\ \dot{\psi}_{s\alpha} = V_{s\alpha} - R_s i_{s\alpha} \\ \dot{\psi}_{s\beta} = V_{s\beta} - R_s i_{s\beta} \\ \dot{\omega}_r = \frac{1}{J} (T_e - T_L) - \frac{f_r \omega_r}{J} \end{cases} \quad (1)$$

with:

$i_{s\alpha}$  and  $i_{s\beta}$  are stator current components respectively,  $\psi_{s\alpha}$  and  $\psi_{s\beta}$  are stator flux components respectively,  $R_s$  and  $R_r$  are stator and rotor resistances respectively,  $L_s$  and  $L_r$  are stator and rotor inductances respectively,  $\omega_r$  is the rotor velocity,  $T_L$  is the load torque,  $J$  is the inertia moment,  $f_r$  is the friction coefficient.

$$\mu = \frac{1}{\sigma} \left( \frac{R_r}{L_r} + \frac{R_s}{L_s} \right), \quad \sigma = 1 - \frac{M_{sr}}{L_s L_r}, \quad T_s = \frac{L_s}{R_s}$$

$M_{sr}$  is the mutual stator-rotor inductance.

The electromagnetic torque is expressed by:

$$T_e = p (\psi_{s\alpha} i_{s\beta} - \psi_{s\beta} i_{s\alpha}) \quad (2)$$

$p$  is the number of pole pairs

## III. DESIGN OF SUPER TWISTING-FEEDBACK LINEARIZATION CONTROL

In order to maintain a fast-decoupled torque control of the IM drive, the chosen control outputs are the electromagnetic torque and the square of stator flux magnitude [6], [13]. The control objectives are defined as:

$$\begin{cases} y_1 = T_e = p (\psi_{s\alpha} i_{s\beta} - \psi_{s\beta} i_{s\alpha}) \\ y_2 = |\psi_s|^2 = \psi_{s\alpha}^2 + \psi_{s\beta}^2 \end{cases} \quad (3)$$

$$\begin{cases} e_1 = T_e^* - T_e \\ e_2 = |\psi_s^*|^2 - |\psi_s|^2 \end{cases} \quad (4)$$

$e_1, e_2$ : torque and flux tracking errors.

The relation between the input and the output can be driven using the presented model in (1) as:

$$\dot{\mathbf{e}} = \begin{bmatrix} \dot{e}_1 \\ \dot{e}_2 \end{bmatrix} = \begin{bmatrix} F_1 \\ F_2 \end{bmatrix} + \mathbf{C}(x) \begin{bmatrix} V_{s\alpha} \\ V_{s\beta} \end{bmatrix} \quad (5)$$

with

$$\begin{cases} F_1 = -p [\mu (\psi_{s\alpha} i_{s\beta} - \psi_{s\beta} i_{s\alpha}) + \omega_r (\psi_{s\alpha} i_{s\alpha} - \psi_{s\beta} i_{s\beta}) \\ \quad - \frac{\omega_r}{\sigma L_s} |\psi_s|^2] \\ F_2 = 2R_s (\psi_{s\alpha} i_{s\alpha} - \psi_{s\beta} i_{s\beta}) \end{cases}$$

$$\mathbf{C}(x) = \begin{bmatrix} -p \left( i_{s\beta} - \frac{\psi_{s\beta}}{\sigma L_s} \right) & p \left( i_{s\alpha} - \frac{\psi_{s\alpha}}{\sigma L_s} \right) \\ -2\psi_{s\alpha} & 2\psi_{s\beta} \end{bmatrix}$$

The determinant of the matrix  $\mathbf{C}(x)$  is expressed as follows:

$$\det(\mathbf{C}(x)) = 2p \frac{M_{sr}}{\sigma L_s L_r} [\psi_{s\beta} \psi_{r\beta} + \psi_{s\alpha} \psi_{r\alpha}] \quad (6)$$

Where:

$\psi_{r\alpha}, \psi_{r\beta}$  are rotor flux components.

As long as the matrix  $\mathbf{C}(x)$  is a non-singular, the system can be called linearizable.

The feedback linearized system will be expressed as:

$$\mathbf{V}_s = \begin{bmatrix} V_{s\alpha}^* \\ V_{s\beta}^* \end{bmatrix} = \mathbf{C}^{-1}(x) \begin{bmatrix} -F_1 + V_1 \\ -F_2 + V_2 \end{bmatrix} \quad (7)$$

$V_1$  and  $V_2$  are presumed auxiliary inputs to ensure more tracking accuracy and desired behavior for the stator flux magnitude and the torque.

$$\begin{cases} V_1 = -k_1 e_1 \\ V_2 = -k_2 e_2 \end{cases} \quad (8)$$

$k_1$  and  $k_2$  are constant gains, they are supposed appropriately positive to have an exponential convergence of the tracking errors [14].

### B. super twisting algorithm

The main advantage of super twisting algorithm (STA) over other high order sliding mode control techniques is that it does not require the time derivatives of sliding variable. This technique can provide a continuous control law by using only the information on the sliding surface [4]. The control law of super twisting  $u_{ST}(t)$  is formed as follows:

$$u_{ST} = u_1(t) + u_2(t) \quad (9)$$

where:

$$\begin{cases} u_1 = -\lambda |S|^\rho \text{sign}(S) + u_1 \\ u_2 = -\int \beta \text{sign}(S) \end{cases} \quad (10)$$

$S$  is the sliding surface.

$\lambda$  and  $\beta$  are positive gains.

$\rho$  is a fractional coefficient between 0 and 0.5 [15].

### C. Super twisting feedback linearization control (STFL)

The proposed design joins the feedback linearization control law with two separated super twisting controllers. The combination of dual nonlinear control strategies can handle the uncertainties and deviation of system parameters. Consequently, it improves its performance and offers a good operation during transient and steady states.

The proposed super twisting controllers receive flux and torque sliding surfaces and produced the auxiliary inputs for the feedback linearization controller.

The sliding surfaces of the flux and torque  $S_{T_e}$  and  $S_{\psi_s}$  are given as:

$$\begin{cases} S_{T_e} = T_e^* - T_e \\ S_{\psi_s} = |\psi_s^*|^2 - |\psi_s|^2 \end{cases} \quad (11)$$

The super twisting torque and flux controllers can be given as follows:

$$\begin{cases} \dot{V}_{T_e} = -\beta \text{sign}(S_{T_e}) \\ V_{ST1} = -\lambda |S_{T_e}|^\rho \text{sign}(S_{T_e}) + V_{T_e} \end{cases} \quad (12)$$

$$\begin{cases} \dot{V}_{\psi_s} = -\beta \text{sign}(S_{\psi_s}) \\ V_{ST2} = -\lambda |S_{\psi_s}|^\rho \text{sign}(S_{\psi_s}) + V_{\psi_s} \end{cases} \quad (13)$$

The sufficient conditions for a finite-time convergence of STA according to [16], [17], are:

$$\begin{cases} \beta > C \\ \lambda^2 > \frac{4C(\beta+C)}{(\beta-C)} \end{cases} \quad (14)$$

where  $C$  is the Lipschitz's constant.

These conditions are necessary for finite-time convergence of STA. However, they may be not enough. Therefore, a strict Lyapunov function for super twisting algorithm's stability is presented by Moreno and Osorio in [18].

The final control law of super twisting feedback linearization (STFL) system (i.e. reference voltages) is expressed as:

$$\mathbf{V}_s = \begin{bmatrix} V_{s\alpha}^* \\ V_{s\beta}^* \end{bmatrix} = \mathbf{C}^{-1}(\mathbf{x}) \begin{bmatrix} -F_1 + V_{ST1} \\ -F_2 + V_{ST2} \end{bmatrix} \quad (15)$$

$V_{ST1}$  and  $V_{ST2}$  are the new super twisting auxiliary inputs

The final reference voltages ( $V_{s\alpha}$ ,  $V_{s\beta}$ ) will be sent to space vector modulation unit in order to generate the inverter switching state under constant switching frequency

#### IV. SUPER TWISTING OBSERVER DESIGN

The sliding mode observers provide high effectiveness due to a number of advantages such as high robustness, simple implementation and reduced computation requirements. The observer is based on the state model of induction motor presented IM in (1).

##### A. Proposed second order sliding mode observer design

By applying the STA to the IM model, a current observer can be constructed as:

$$\begin{cases} \dot{\hat{i}}_{s\alpha} = -\mu \hat{i}_{s\alpha} - \hat{\omega}_r \hat{i}_{s\beta} + \frac{1}{\sigma L_r} \left( \frac{\hat{\psi}_{s\alpha}}{T_s} + \hat{\omega}_r \hat{\psi}_{s\beta} \right) + \frac{V_{s\alpha}}{\sigma L_s} + u_1(S_{is\alpha}) \\ \dot{\hat{i}}_{s\beta} = -\mu \hat{i}_{s\beta} + \hat{\omega}_r \hat{i}_{s\alpha} + \frac{1}{\sigma L_r} \left( \frac{\hat{\psi}_{s\beta}}{T_s} - \hat{\omega}_r \hat{\psi}_{s\alpha} \right) + \frac{V_{s\beta}}{\sigma L_s} + u_1(S_{is\beta}) \end{cases}$$

(16)

In this proposed second order sliding mode observer, the chosen switching surfaces  $S_i$  is stator current estimation error.

$$\begin{cases} S_{is\alpha} = i_{s\alpha} - \hat{i}_{s\alpha} \\ S_{is\beta} = i_{s\beta} - \hat{i}_{s\beta} \end{cases} \quad (17)$$

Then, the flux observer can be defined as:

$$\begin{cases} \dot{\hat{\psi}}_{s\alpha} = V_{s\alpha} - R_s i_{s\alpha} + u_2(S_{is\alpha}) \\ \dot{\hat{\psi}}_{s\beta} = V_{s\beta} - R_s i_{s\beta} + u_2(S_{is\beta}) \end{cases} \quad (18)$$

where  $u_1$  and  $u_2$  are additional design parameters which are defined as:

$$\begin{cases} u_1 = -\lambda |S|^\rho \text{sign}(S_i) \\ u_2 = -\int \beta \text{sign}(S_i) \end{cases} \quad (19)$$

The conditions of super twisting-observer converge in finite time can be done in similar way as shown in (14) [12].

The diagram shown in Fig.1 presents the design of proposed second order sliding mode current and flux observer.

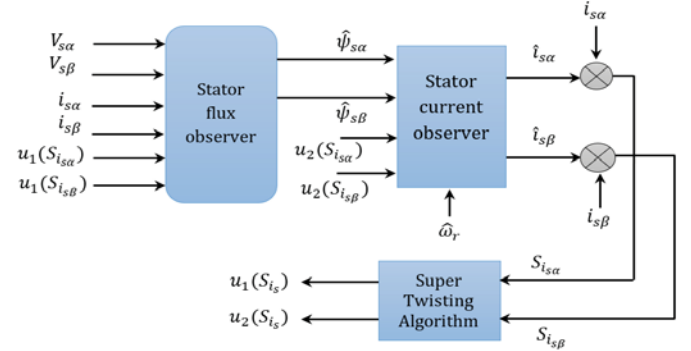


Fig.1 Super twisting based current and flux observer.

##### B. Speed estimation

The estimated speed quantity in the proposed observer is obtained by MRAS approach. The MRAS structure consists of two parts, the reference model and the adaptive model, in addition to the adaptation mechanism [19]. In this work, the proposed super twisting observer will serve as a reference model. Then, the estimated flux quantities will be compared to those estimated by MRAS's adaptive model.

The adjustable model is expressed as follows:

$$\begin{cases} \tilde{\psi}_{s\alpha} = \frac{L_r}{R_r + L_r s} \left( \sigma L_s \hat{\omega}_r i_{s\beta} + \frac{L_s}{L_r} (R_r + \sigma L_r s) i_{s\alpha} - \hat{\omega}_r \tilde{\psi}_{s\beta} \right) \\ \tilde{\psi}_{s\beta} = \frac{L_r}{R_r + L_r s} \left( \sigma L_s \hat{\omega}_r i_{s\alpha} + \frac{L_s}{L_r} (R_r + \sigma L_r s) i_{s\beta} - \hat{\omega}_r \tilde{\psi}_{s\alpha} \right) \end{cases} \quad (20)$$

The error between the estimated quantities using ST-Observer reference and the adaptive mode can be given by:

$$\begin{cases} \varepsilon_\alpha = \hat{\psi}_{s\alpha} - \tilde{\psi}_{s\alpha} \\ \varepsilon_\beta = \hat{\psi}_{s\beta} - \tilde{\psi}_{s\beta} \end{cases} \quad (21)$$

The error used to drive a suitable adaptation mechanism to generates the estimated speed quantity [20]. The estimated speed is given as:



$$\hat{\omega}_r = K_p \varepsilon + K_i \int \varepsilon dt \quad (22)$$

where  $\varepsilon$  is the estimation error expressed as:

$$\varepsilon = (\hat{\psi}_s \beta \tilde{\psi}_{s\alpha} - \hat{\psi}_{s\alpha} \tilde{\psi}_{s\beta} - (\hat{i}_{s\alpha} \varepsilon_\beta - \hat{i}_{s\beta} \varepsilon_\alpha) \sigma L_s) \quad (23)$$

Fig.2 shows the full MRAS-Super twisting observer design.

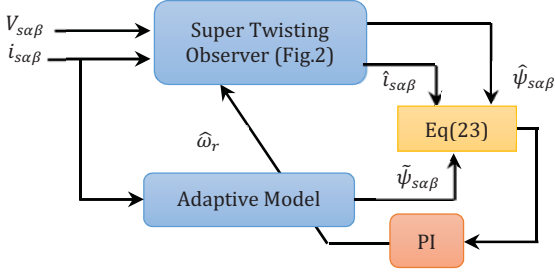


Fig.2 Association of Stator Flux model-MRAS speed observer with SMO

To implement the global sensorless control algorithm, the flux observer must be initialized firstly with initial conditions different from zero in order to avoid the singularity. Therefore, an offset of 0.005Wb is added to the estimated flux.

The global diagram of super twisting-feedback linearization sensorless control based on MRAS-super twisting observer is shown in Fig.3.

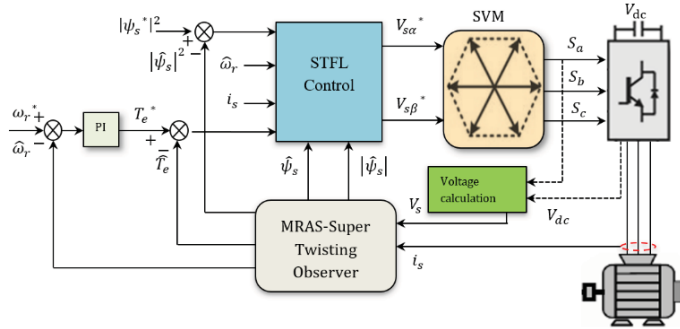


Fig.3 Block diagram of STFL-direct torque control with space vector modulation.

## V. EXPERIMENTAL RESULTS

### A. Experimental setup presentation

The implementation of super twisting feedback linearization with super twisting observer has been done using MATLAB/Simulink software with dSpace 1104 real-time interface.



Fig.4 Test bench description.

The shown experimental test bench in Fig.4 consists of: 1: A 1.1 kW squirrel-cage induction machine, 2: two-level power electronics voltage converter, 3: an incremental encoder, 4:

dSpace 1104 real-time interface, 5: personnel computer with MATLAB/Simulink/ControlDesk software, 6: magnetic powder brake, 7: Hall effect current sensors, 8: voltage sensors. 9: digital oscilloscope. The diagram shown in Fig.5 describe the software hardware linking.

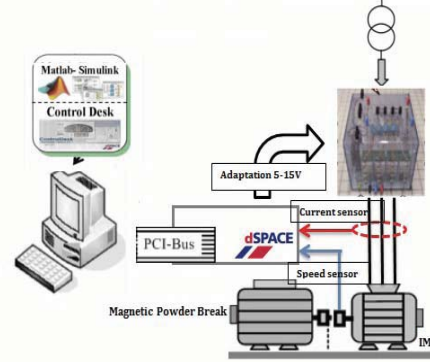


Fig. 5 descriptive diagram

### B. STFL Control performance analysis: Steady state, load application and speed reversal

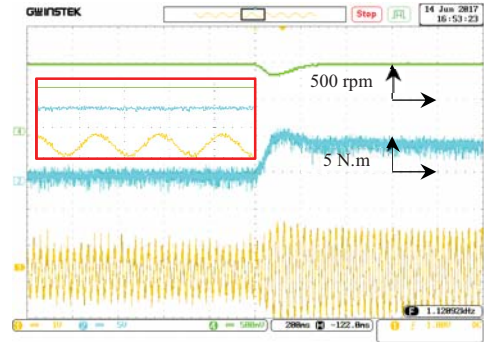


Fig.6 Steady state and load application: Rotor speed, load torque, current.

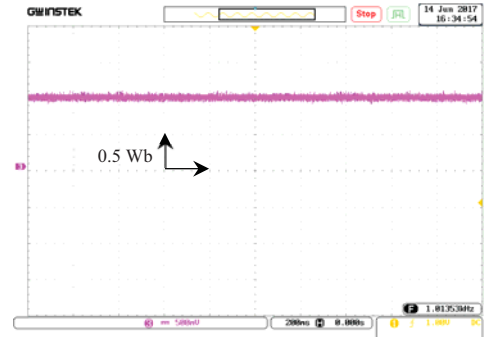


Fig.7 Steady state: stator flux magnitude.

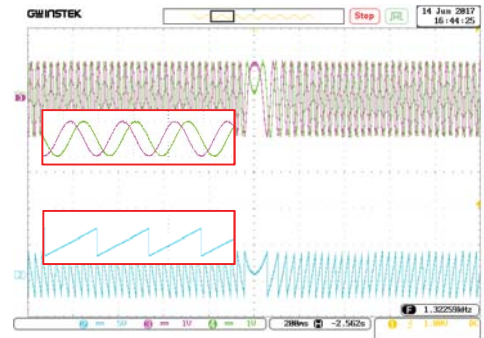


Fig.8 Speed sense reversal: Stator flux components, flux position

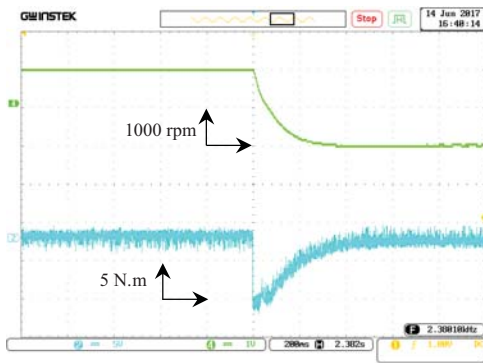


Fig.9 Speed sense reversal: Rotor speed, electromagnetic torque

Fig.6 shows the steady state followed by load application of 5N.m, the figure presents from top to bottom: rotor speed, electromagnetic torque and stator current. The rotor speed tracks its reference (1000 rpm) perfectly, while the drop due to load has been recovered quickly. The torque and stator current also show a smooth waveform and reduced ripples due to the use of SVM that preserve a fixed switching frequency and reduce ripples and harmonics. Next, Fig.7 presents the stator flux magnitude following its reference 1 Wb. Besides, the good flux tracking, it shows a reduced ripples level also. Then, in Fig.8, the stator flux components are illustrated, it can be seen that the flux evolution has a pure sinusoids waveform due to proposed direct flux control. The flux position below has been added to indicated the sense changing direction. Finally, a speed reversal test is shown in Fig.9. The figure presents the rotor speed and torque during the reversing phase, this test has been conducted in order to test the control dynamic and response. It can be concluded that the proposed STFL control algorithm has a good dynamic and tracking

*C. MRAS-Super Twisting observer performance analysis: Transient state, low speed operation, variable speed.*

This section presents the performance analysis of the proposed super twisting second-order sliding mode observer with MRAS. Various speed tests have been performed in order to check the observer abilities in wide speed range.

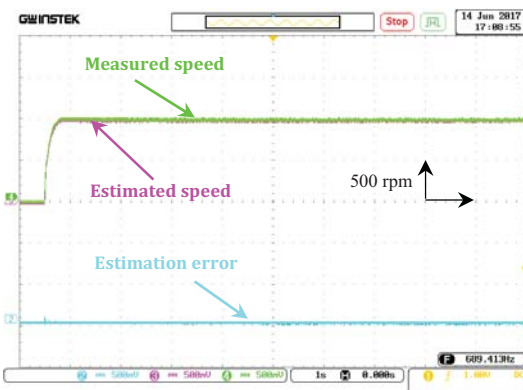


Fig.10 Starting up: Measured and estimated speed, estimation error.

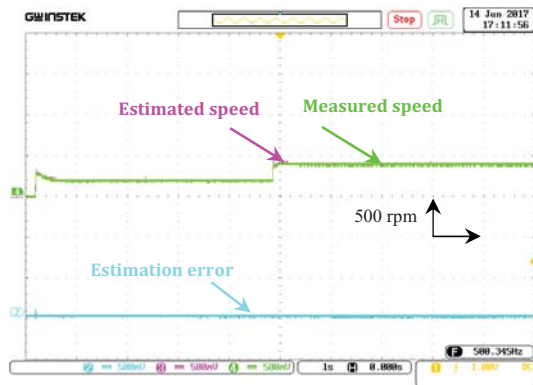


Fig.11 Low speed operation: Measured and estimated speed (200-400 rpm), estimation error

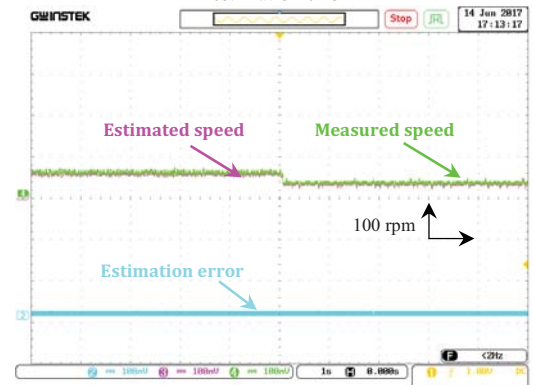


Fig.12 Low speed operation: Measured and estimated speed (50-25 rpm), estimation error

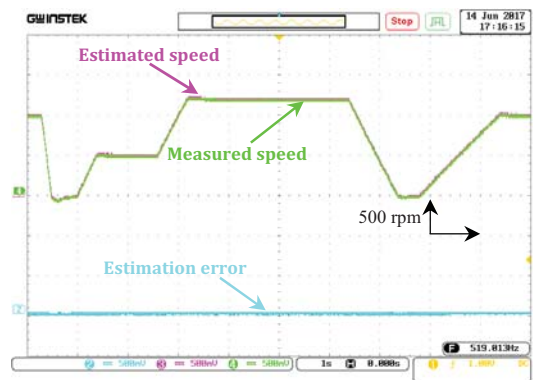


Fig.13 Variable speed operation: Measured and estimated speed, estimation error.

Fig.10 presents the starting up state of the motor, two speed quantities (i.e. measured using encoder and estimated using ST-Observer) have been compared and the estimated error has been computed. It can be seen that the two speed quantities show full superposition while the estimation error converge quickly to zero. In Figs.11-12, low speed operation has been performed, a speed reference variation from 200-400 rpm and 50-25 rpm are presented respectively in Fig.11 and Fig.12. A small overshoot has arisen at the beginning in Fig.11 but it has been recovered quickly. Then, in steady state the estimated and measured speed quantities show a full superposition, while the estimation error converges instantly to zero. Moreover, this can be seen also in very load speed region in Fig.12 (50-25 rpm), where the estimation accuracy has been kept, the speed shows no

fluctuations and the control stability is preserved. Finally, in Fig.13, a variable speed test has been performed. This test can comprise all the previous tests, it shows the rotor speed estimation and estimation errors in zero to medium speed (500 rpm) then to high-speed value (1200 rpm). It can be noticed that the proposed super twisting observer associated to MRAS. it provides good estimation and perfect speed superposition during the instant speed variations, also a reduced estimation error in dynamic state operation and very quick convergence in steady state.

## VI. CONCLUSION

This work proposed a novel performance enhancement on induction motor flux and torque control using dual nonlinear control approaches. The combined control strategy has been applied in order to solve different drawbacks of the classical control scheme. The decoupled control has been realized using feedback linearization approach to generate the reference voltages. Then, the super twisting algorithm has been integrated as a supporter auxiliary control to achieve the so-called robust feedback linearization control.

The investigation of the proposed algorithm has been done under different operation conditions through experimental implementation using dSpace 1104. Moreover, the proposed super twisting observer has been tested also, it shows good estimation accuracy in different speed regions that reflect on the overall system reliability cost. Generally, the application of the continuous super twisting for control and estimation provide reduced chattering, fast dynamic, high robustness and good estimation in wide speed region. Besides, it has kept the simplicity of control design as much as possible.

## APPENDIX

The parameters of the used three-phase Induction motor, in SI units are:

$1.1kW$ ,  $50\text{ Hz}$ ,  $p=2$ ,  $R_s=6.75\Omega$ ,  $R_r=6.21\Omega$ ,  $L_s=L_r=0.5192\text{ H}$ ,  $M_{sr}=0.4957\text{ H}$ ,  $f_i=0.002\text{ N}\cdot\text{m}\cdot\text{s}$ ,  $J=0.01240\text{ kg}\cdot\text{m}^2$ .

The sampling frequency :10 kHz.

inverter's switching frequency: 5 kHz.

DC link voltage:  $V_{dc}= 537\text{ V}$ .

## REFERENCE

- [1] F. Wang, Z. Zhang, X. Mei, J. Rodríguez, and R. Kennel, "Advanced control strategies of induction machine: Field oriented control, direct torque control and model predictive control," *Energies*, vol. 11, no. 1, 2018.
- [2] D. Casadei, F. Profumo, G. Serra, and A. Tani, "FOC and DTC: Two viable schemes for induction motors torque control," *IEEE Trans. Power Electron.*, vol. 17, no. 5, pp. 779–787, 2002.
- [3] C. Lascu, I. Boldea, and F. Blaabjerg, "A modified direct torque control for induction motor sensorless drive," *IEEE Trans. Ind. Appl.*, vol. 36, no. 1, pp. 122–130, 2000.
- [4] A. Ammar, "Second-order sliding mode-direct torque control and load torque estimation for sensorless model reference adaptive system-based induction machine," *Proc. Inst. Mech. Eng. Part I J. Syst. Control Eng.*, p. 095965182093569, Jul. 2020.
- [5] Y. Fang, J. Fei, and T. Hu, "Adaptive backstepping fuzzy sliding mode vibration control of flexible structure," *J. Low Freq. Noise, Vib. Act. Control*, p. 146134841876709, Mar. 2018.
- [6] A. Ammar, A. Kheldoun, B. Metidji, and T. Ameid, "Feedback linearization based sensorless direct torque control using stator flux MRAS-sliding mode observer for induction motor drive," *ISA Trans.*, vol. 98, pp. 382–392, 2020.
- [7] Z. Zhang, R. Tang, B. Bai, and D. Xie, "Novel Direct Torque Control Based on Space Vector Modulation With Adaptive Stator Flux Observer for Induction Motors," *IEEE Trans. Magn.*, vol. 46, no. 8, pp. 3133–3136, Aug. 2010.
- [8] R. N. Mishra and K. B. Mohanty, "Real time implementation of an ANFIS-based induction motor drive via feedback linearization for performance enhancement," *Eng. Sci. Technol. an Int. J.*, vol. 19, no. 4, pp. 1714–1730, Dec. 2016.
- [9] C. Lascu, S. Jafarzadeh, M. S. Fadali, and F. Blaabjerg, "Direct Torque Control With Feedback Linearization for Induction Motor Drives," *IEEE Trans. Power Electron.*, vol. 32, no. 3, pp. 2072–2080, Mar. 2017.
- [10] M. Zaidabadi nejad and G. R. Ansarifar, "Robust feedback-linearization control for axial power distribution in pressurized water reactors during load-following operation," *Nucl. Eng. Technol.*, vol. 50, no. 1, pp. 97–106, Feb. 2018.
- [11] M. H. Holakooie, M. Ojaghi, and A. Taheri, "Modified DTC of a Six-Phase Induction Motor With a Second-Order Sliding-Mode MRAS-Based Speed Estimator," *IEEE Trans. Power Electron.*, vol. 34, no. 1, pp. 600–611, Jan. 2019.
- [12] Lihang Zhao, Jin Huang, He Liu, Bingnan Li, and Wubin Kong, "Second-Order Sliding-Mode Observer With Online Parameter Identification for Sensorless Induction Motor Drives," *IEEE Trans. Ind. Electron.*, vol. 61, no. 10, pp. 5280–5289, Oct. 2014.
- [13] T. Orłowska-Kowalska, G. Tarchala, and M. Dybkowski, "Sliding-mode direct torque control and sliding-mode observer with a magnetizing reactance estimator for the field-weakening of the induction motor drive," *Math. Comput. Simul.*, vol. 98, pp. 31–45, 2014.
- [14] Y.-S. Choi, H. H. Choi, and J.-W. Jung, "Feedback Linearization Direct Torque Control With Reduced Torque and Flux Ripples for IPMSM Drives," *IEEE Trans. Power Electron.*, vol. 31, no. 5, pp. 3728–3737, May 2016.
- [15] M. Rashed, K. B. Goh, M. W. Dunnigan, P. F. A. MacConnell, A. F. Stronach, and B. W. Williams, "Sensorless second-order sliding-mode speed control of a voltage-fed induction-motor drive using nonlinear state feedback," *IEE Proc. - Electr. Power Appl.*, vol. 152, no. 5, p. 1127, 2005.
- [16] A. Levant, "Higher-order sliding modes, differentiation and output-feedback control," *Int. J. Control*, vol. 76, no. 9–10, pp. 924–941, 2003.
- [17] A. Levant, "Robust Exact Differentiation via Sliding Mode Technique," *Automatica*, vol. 34, no. 3, pp. 379–384, 1998.
- [18] J. A. Moreno and M. Osorio, "Strict Lyapunov Functions for the Super-Twisting Algorithm," *IEEE Trans. Automat. Contr.*, vol. 57, no. 4, pp. 1035–1040, Apr. 2012.
- [19] G. Tarchala and T. Orłowska-Kowalska, "Equivalent-Signal-Based Sliding Mode Speed MRAS-Type Estimator for Induction Motor Drive Stable in the Regenerating Mode," *IEEE Trans. Ind. Electron.*, vol. 65, no. 9, pp. 6936–6947, Sep. 2018.
- [20] C. Schauder, "Adaptive speed identification for vector control of induction motors without rotational transducers," *IEEE Trans. Ind. Appl.*, vol. 28, no. 5, pp. 1054–1061, 1992.